

# **Enhancement of Organic Solar Cell Performance through Solvent Annealing**

Senior Honors Thesis

Department of Chemical and Biological Engineering

Derrick M. Kane

Tufts University 2013

## ACKNOWLEDGEMENTS

First, I would like to thank Professor Matthew Panzer for encouraging me to pursue a senior honors thesis, and providing me with the means to do so. I would also like to extend my appreciation to the rest of the Green Energy and Nanostructured Electronics (GENE) Lab for providing a supportive research environment.

Second, I would like to thank Professor Tom Vandervelde and his lab group for the use of his solar simulator, the use of which was crucial to this research.

Third, I would like to thank Professor Ayse Asatekin, and my classmate and fellow thesis candidate John Abel, for their advice concerning the Hildebrand solubility parameter. John's Hildebrand solubility parameter calculator in Microsoft Excel was exceptionally useful in expediting the approximation of the solubility parameter of CuPc.

Last, I would like to extend my thanks to the Chemical and Biological Engineering Department at Tufts University for being supportive and eager to assist in any way possible with my thesis topic.

# TABLE OF CONTENTS

Acknowledgements.....	ii
List of Figures.....	v
List of Tables.....	v
Abstract.....	vi
1 Introduction.....	1
1.1 Overview.....	1
1.2 Background.....	1
1.3 Materials.....	3
1.4 Objectives.....	4
2 Experimental Methods.....	5
2.1 Device Cleaning and Preparation.....	5
2.2 Device Fabrication.....	5
2.3 Device Testing.....	7
3 Results and Discussion.....	8
3.1 AFM Imaging.....	8
3.2 Acetone Vapor Treatment.....	9
3.3 Solubility Parameter Approximation.....	13
3.4 Other Solvent Results.....	16
4 Conclusions.....	17
5 Future Studies.....	18

Bibliography .....	20
Appendix A.....	22
Appendix B .....	23

## LIST OF FIGURES

Figure 1.2.1 - Organic Photovoltaics Heterojunction Morphologies.....	2
Figure 1.3.1 - OPV Device Energy Diagram.....	4
Figure 2.2.1 - OPV Device Structure.....	6
Figure 3.1.1 - AFM Images of Acetone Treated CuPc Films.....	9
Figure 3.2.1 - Efficiency Optimization by Acetone Vapor Treatment.....	10
Figure 3.2.2 - Acetone Treated Devices, Open Circuit Voltage & Fill Factor.....	12
Figure 3.2.3 - Acetone Treated Devices, Short Circuit Current Density.....	12
Figure 3.4.1 - AFM Images of Other Solvent Treatments.....	16

## LIST OF TABLES

Table 3.2.1 - Analysis of Acetone Vapor Treatments.....	11
Table 3.3.1 - Approximation of the Hildebrand Solubility Parameter for CuPc.....	15
Table 3.3.2 - Hildebrand Solubility Parameters for Common Solvents.....	15
Table 3.4.1 - Analysis of Other Solvent Treatments.....	16
Table 3.4.2 - Vapor Pressure of Treatment Solvents.....	17

## ABSTRACT

Copper phthalocyanine (CuPc) has shown promise in organic thin film electronics applications due to its ability to crystallize into ordered nanorods when exposed to solvent. In this study, CuPc nanostructured films were created through thermal evaporation of CuPc and subsequent treatment with acetone vapor for use in organic photovoltaic (OPV) cells. AFM imaging was used to confirm the growth of the nanorods, which were observed to form after 15 min of treatment and achieve a height of 50 nm after 20 min. Maximum power conversion efficiency obtained was 0.534%, a 46.5% improvement versus the untreated cell. Efficiencies achieved were significantly lower than previously reported CuPc:PCBM devices in which the acceptor layer (PCBM) was applied by solution processing (typical efficiency 1.5-3.0%). Although CuPc nanorod growth was found to increase surface roughness with increased treatment time, short circuit current density was not statistically improved. Deposition of the acceptor layer by thermal evaporation may have inadequately filled the CuPc nanostructure spacing due to 3D shadowing effects of the CuPc nanorods, and allowed the 50 nm nanorods to bridge the active layer and cause current leakage.

Furthermore, the Hildebrand solubility parameter,  $\delta$ , was studied as a useful solvent property to correlate with a solvent's effectiveness for CuPc nanorod growth. Using Fedors' group contribution method, the solubility parameter of CuPc was approximated to be  $25.09 \text{ MPa}^{1/2}$ , with possible error due to the lack data for the copper atom. Ethanol ( $\delta = 26.0 \text{ MPa}^{1/2}$ ) was chosen as a solvent predicted to have high CuPc solubility, compared to acetone ( $\delta = 20 \text{ MPa}^{1/2}$ ). In case of an underestimate, dimethyl sulfoxide (DMSO) ( $\delta = 29.7 \text{ MPa}^{1/2}$ ) was selected as upper bound. Ethanol and DMSO treatments were applied to CuPc films for 15 min. DMSO was found to raise device efficiency to 0.505%, with promising effects on fill factor and surface roughness. Advice regarding further study of DMSO treatment is included.

# 1 INTRODUCTION

## 1.1 OVERVIEW

The demand for a sustainable, environmentally-friendly energy source has spurred research in the field of organic photovoltaics (OPVs) in recent years. OPV cells have many traits that make them appealing when compared to conventional silicon solar cells. In general, the organics in OPV devices have much higher absorption coefficients than silicon, so films can be made thinner (100s of nm vs. 100s of  $\mu\text{m}$ ) [1,2]. These organic devices use small quantities of material, low energy input, and are easily processed by solution methods, including scale-up methods by roll-to-roll processing [2].

Current density is a parameter that needs improvement in organic photovoltaics. Organic solar cells have not been able to achieve efficiencies as high as inorganic or dye-sensitized solar cells, in part due to the loss of current to recombination [2]. To remedy this situation, much attention has been given to methods of nanostructuring organic thin films to improve device current by reducing losses to recombination. In particular, solvent annealing has been examined as a means of creating an ordered surface [3,4,5].

## 1.2 BACKGROUND

The mechanism by which an OPV creates current from light is a complex one, involving several steps and opportunities for efficiency loss. OPV cells are in general composed of two conjugated small-molecule organic compounds, termed the donor and accept layers. These organic layers, together called the active layer, are sandwiched between two electrodes. The absorption of a photon by a pi electron in a conjugated bond of the electron donor layer causes excitation of the electron into a high energy state [6]. This photoexcitation causes the generation of an electron-hole pair held together by electrostatic forces, referred to as an exciton. The columbic energy between the positive and negative charges must be smaller than the energy gap between the Highest Unoccupied Molecular Orbital (HOMO) of the donor and Lowest Unoccupied Molecular Orbital (LUMO) of the acceptor in order for the separation of charges to

be energetically favorable [6]. The exciton diffuses through the donor material until it reaches the donor-acceptor interface or recombination of the electron-hole pair occurs. Recombination represents both a loss of current, and a decrease in the device voltage. At the donor-acceptor interface, separation of charges occurs. Next, the electron and hole are transported through the acceptor and donor layers, respectively, and charges are collected at the electrodes. This concludes the generation of current in an OPV cell.

The morphology of the donor-acceptor interface, sometimes called the heterojunction, is an important consideration in the creation of an OPV. Three main morphologies exist: bilayer heterojunction, bulk heterojunction, and the ideal heterojunction. Since typical diffusion lengths for organics range from 1-10 nm for organics [3] - small compared to device thicknesses which can be as high as 100 nm - reducing the required diffusion path length to the donor-acceptor interface can dramatically reduce the effect of exciton recombination. Figure 1.2.1 demonstrates the different heterojunction morphologies.

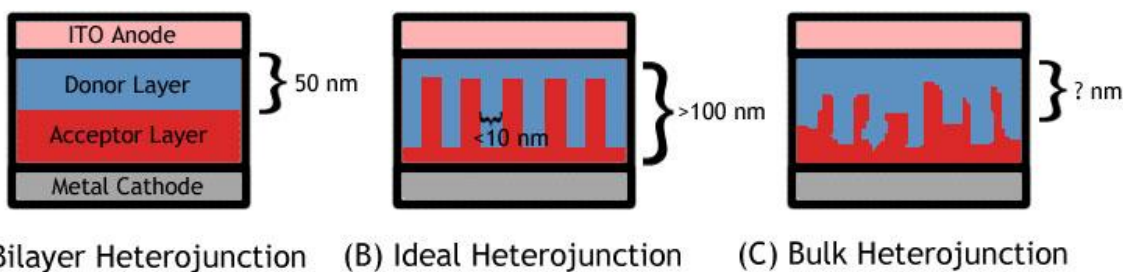


**Figure 1.2.1** - Organic Photovoltaic Device Morphologies.

In the simplest device morphology, the bilayer heterojunction, the donor and acceptor are both deposited as planar layers, causing the path length to be very high unless the active layer is made very thin. However, a thin active layer cannot absorb light as completely, so there is a trade off. One solution is the bulk heterojunction, where the active layer is deposited from a single solution, and phase separation causes the interface to become a random interpenetrating network of donor and acceptor [7]. This serves to reduce the distance from a given point in the donor layer to the interface, and reduce recombination. The limitation of this method is controllability. Characterizing the interface, or more importantly,



controlling it, becomes difficult. Isolated areas of donor and acceptor can become suspended, without a path for the carriers to travel to the electrodes. The perfect implementation of a bulk-heterojunction-like design would be to create a system of interpenetrating rods with a regular spacing less than or equal to the diffusion length for the polymer used. This would lead to the ideal heterojunction. While the ideal heterojunction is not easy to achieve, it can be approximated by certain printing techniques or surface treatments.

### 1.3 MATERIALS

Copper (II) phthalocyanine (CuPc) exhibits many useful electrical properties which make it the subject of this thesis. Studies have shown that CuPc is capable of growing single-crystal nanorods in the presence of solvent due to the pi-pi stacking of the phthalocyanine groups [3]. It has been shown that growth of these crystalline nanorods occurs during the evaporation of the solvent from the film surface [4]. Interestingly, these nanorods have diameters that are on the same order of magnitude as the exciton diffusion length of CuPc (several tens of nanometers) [3]. Vertically aligned CuPc nanorods could be exploited to create an OPV cell the morphology of which approximates the ideal heterojunction. Efforts have been made to incorporate this feature into organic photovoltaics and to optimize nanorod growth using a variety of solvents for CuPc treatment, including chloroform, chlorobenzene, toluene, and acetone [4,8]. Of these solvents, acetone was discovered to cause the most vertical nanorod growth, high CuPc surface roughness, and increased absorbance of the CuPc layer over the visible range [8]. Several methods of solvent treatment have been examined, including CuPc crystal growth by solution deposition, solvent drop, and solvent vapor annealing [3,5,8]. Solvent annealing with acetone vapor has been proven to cause significant nanorod growth, but has not yet been implemented in photovoltaic applications [5].

The rest of the materials in the device structure examined in this thesis were selected for their standard use in OPV cells. Poly(3,4-ethylenedioxythiophene):poly(styrenesulfonate) (PEDOT:PSS) has been selected as a wide band-gap electron-blocking layer, and serves to provide a planar surface atop the

Indium Tin Oxide (ITO) anode. Bathocuproine has been selected as an hole-blocking layer, a buffer to protect the active layer against the thermal deposition of the aluminum cathode, and to remain consistent with previous CuPc OPV cell architectures [8,9]. Finally, buckminsterfullerene ( $C_{60}$ ) was chosen as the acceptor material, rather than PCBM, due to its ability to be deposited by thermal deposition rather than solution processing, which is discussed further in the next section.

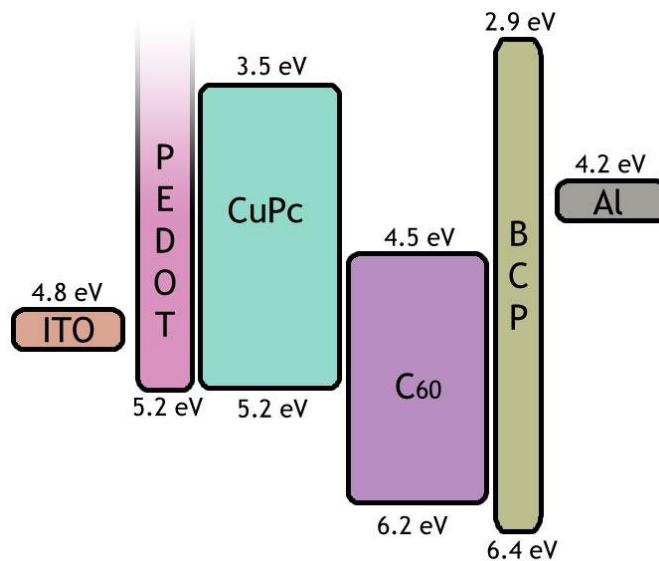


Figure 1.3.1 - Energy Diagram

## 1.4 OBJECTIVES

In this thesis, the creation of an OPV cell in approximation of the ideal heterojunction was sought through the growth of CuPc nanorods by solvent annealing with acetone vapor. Unlike other CuPc nanostructured OPV cell studies, the acceptor layer ( $C_{60}$ ) was deposited using dry methods, namely thermal evaporation. Previous studies of CuPc:PCBM cells have used solution methods (i.e. spin-coating) to deposit the acceptor layer, which use chlorobenzene as a solvent [8]. The same study uses chlorobenzene as a solvent for nanorod growth, which provokes one to question whether the nanostructured surface is affected, or even damaged, by the deposition of the acceptor layer. This thesis aims to preserve the nanostructured surface by depositing the subsequent layers by thermal evaporation, rather than spin-coating.

Other than observation of the treated surface and characterization of treated devices, little analysis has been done to determine what solvent properties determine quality of the CuPc nanostructure and crystal growth during solvent annealing. For this purpose, an examination of the solvent properties that cause CuPc nanorod growth was conducted. Approximation of the Hildebrand solubility parameter for CuPc was chosen as a means for selecting feasible annealing solvents, from which ethanol and dimethyl sulfoxide (DMSO) were chosen. These solvents served as reasonable mid and upper solubility parameter values to compliment the already conducted acetone treatment. Suggestions for the further study of the solubility of CuPc, and device fabrication experiments regarding DMSO have been included.

## 2 EXPERIMENTAL METHODS

### 2.1 DEVICE CLEANING AND PREPARATION

All solar devices were prepared on glass substrates pre-patterned with a  $145\pm 10$  nm ITO anode from Thin Film Devices Inc. Each substrate was subjected to a cleaning procedure prior to thin film deposition. The glass-ITO substrates were washed in a four step method. Each step used roughly 80 ml of solvent and lasted 5 minutes. The first three steps were performed at room temperature in an ultrasonicator with the following solvents: 0.2% Micro-90 soap solution, deionized water, and acetone. The last step was a bath in boiling isopropyl alcohol (boiling point:  $82.5^{\circ}\text{C}$ ). After the final solvent bath, the substrates were dried with a burst of nitrogen gas before being stored.

In order to obtain a smooth layer of PEDOT:PSS, the substrates were made more hydrophilic before application of the thin film. Just before the spin-coating of PEDOT:PSS, the substrates were bathed in an 80 ml solution of 1M sodium hydroxide for a half hour.

### 2.2 DEVICE FABRICATION

Thin films were deposited using two methods: spin-coating and thermal evaporation. The device structure shared by all devices is shown in Figure 2.2.1.

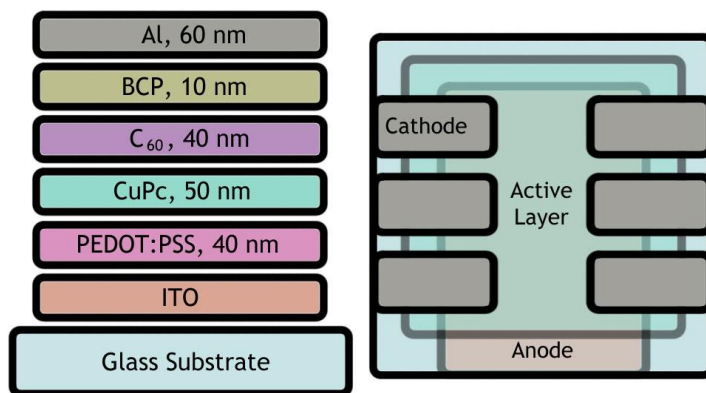


**Figure 2.2.1** - OPV Device Structure: Cross-sectional view (left) and simplified underside view (right).

First, the PEDOT:PSS layer was deposited by spin-coating. The water-based solution was applied to the surface by syringe and passed through a 0.45  $\mu\text{m}$  PTFE filter. A spin speed of 3000 rpm for 1 minute was selected, and yielded a 40 nm film thickness (confirmed by AFM imaging). The coated substrates were then heated in open air on a hotplate at 150°C for 20 minutes. This ensured that any remaining water would evaporate off before the cells were brought into the nitrogen-atmosphere glove boxes.

Next, the devices were brought into the glove-box for thermal deposition of the CuPc layer. Under high vacuum ( $\sim 10^{-6}$  mbar), >99.99% triple-sublimed grade CuPc from Sigma Aldrich was deposited at a rate of  $\sim 1$  Å/s through a square shadow mask (see Appendix A). Thickness was recorded by Quartz Crystal Monitor during deposition. Once the CuPc thin film was applied, devices were removed again from the glove-boxes and treated by solvent annealing.

The solvent annealing process involved sealing the devices with the CuPc layer exposed to solvent vapors. In a fume hood under ambient conditions, 5 ml of solvent was added to a Petri dish (enough to coat the bottom). For most tests, the solvent was acetone, but later tests involved ethanol and DMSO. Each cell was placed face-up in the Petri dish on an inert plastic stage to elevate it above the liquid. A lid was then placed over the dish to seal the cell in with the solvent vapors, and the chamber was allowed to

sit for the duration of its treatment. Once the treatment time was over, the cell was removed, rinsed briefly with a nitrogen gas stream, and transported back into the glove-box. Devices made for surface imaging were instead taken directly to the AFM after this treatment.

The remaining layers were deposited in the thermal evaporation chamber. TDK-Lambda power sources were used; 100A source for C<sub>60</sub>, and 200A sources for the BCP and aluminum. The >99.5% C<sub>60</sub> was deposited through the square shadow mask at a rate of ~1.0 Å/s. The BCP (99.99% sublime grade, Sigma Aldrich) was deposited at a rate of ~1.0 Å/s as well. The Al (>99.999% evaporation slug, Sigma Aldrich) was deposited at rates between ~1.0-10.0 Å/s, due to the tendency of aluminum to fluctuate heating rate rapidly. Both BCP and Al were deposited through a separate shadow mask for six electrodes per cell (see Appendix A).

### 2.3 DEVICE TESTING

Each cell was loaded into a custom testing apparatus before being brought out of the glove. The testing apparatus included an inset stage for the cell with six gold pins to contact the six aluminum cathodes (see Appendix A). The cell was tightened down, and its connectivity verified with a Keithley 2602A SourceMeter by measuring current under ambient light. Once the cell was properly connected, the apparatus lid was clamped down and sealed under nitrogen. The lid included a window to allow light to enter the apparatus.

The contained devices were removed from the glove boxes and tested with a Newport Oriel Solar Simulator. The Solar Simulator was fitted with a 1600W Xenon Arc Lamp and an optical filter (optical density 1.0 @632.8 nm) to reduce the incident light to an intensity of 1 sun AM1.5 (100 mW/cm<sup>2</sup>). The incident light was measured and entered into the Oriel software prior to testing each cell, and in practice usually measured between 0.8-1.0 sun AM1.5. Device response was analyzed by another Keithley SourceMeter and Oriel PVIV Software in LabVIEW. The software automatically determined the open

circuit voltage, short circuit current density, fill factor, resistances, and power conversion efficiency from the collected IV data using standard equations [5].

## 3 RESULTS AND DISCUSSION

### 3.1 AFM IMAGING

The treated CuPc films were examined by tapping mode Atomic Force Microscope (AFM) imaging, as seen in Figure 3.1.1. An image of a 15 min acetone treatment can also be found in Figure 3.4.1. All AFM images shown here are  $1.5\ \mu\text{m} \times 1.5\ \mu\text{m}$  squares, with a 50 nm color scale. The untreated CuPc film was mostly planar, but with a faint bead-like surface that is typical of thermally evaporated films. As the duration of the acetone solvent treatments increase, the beads merge into oblong structures, which become nanorods at times longer than  $\sim 15$  min. In the 20 min image, peaks roughly 50 nm high have formed; however, most nanorods appear to be laying horizontal, as previous studies have found occurs with other solvents such as toluene or chloroform [4,8]. It has been reported in another study that nanorods grown by solvent annealing with acetone vapor in nitrogen carrier gas display a mix of vertical and horizontal nanorods [4]. One possible explanation is that treatment by solvent drop, due to the relatively large quantity of liquid coating the CuPc surface, allows the dissolved CuPc particles to move more freely in three dimensions, and thus causes increased growth of vertical nanorods. The fact that nanorod size increases with larger drop volumes support this [3]. In this method, the amount of solvent that collects on the surface from vapor is much smaller. In the nitrogen carrier gas study, the nitrogen was bubbled through acetone to obtain a higher ambient concentration of acetone, thus causing increased solvent interaction with the surface compared to the level that ambient vapor pressure would achieve. Additionally, since the treatment was performed in open air, ambient conditions such as humidity, may have caused interfering surface effects.

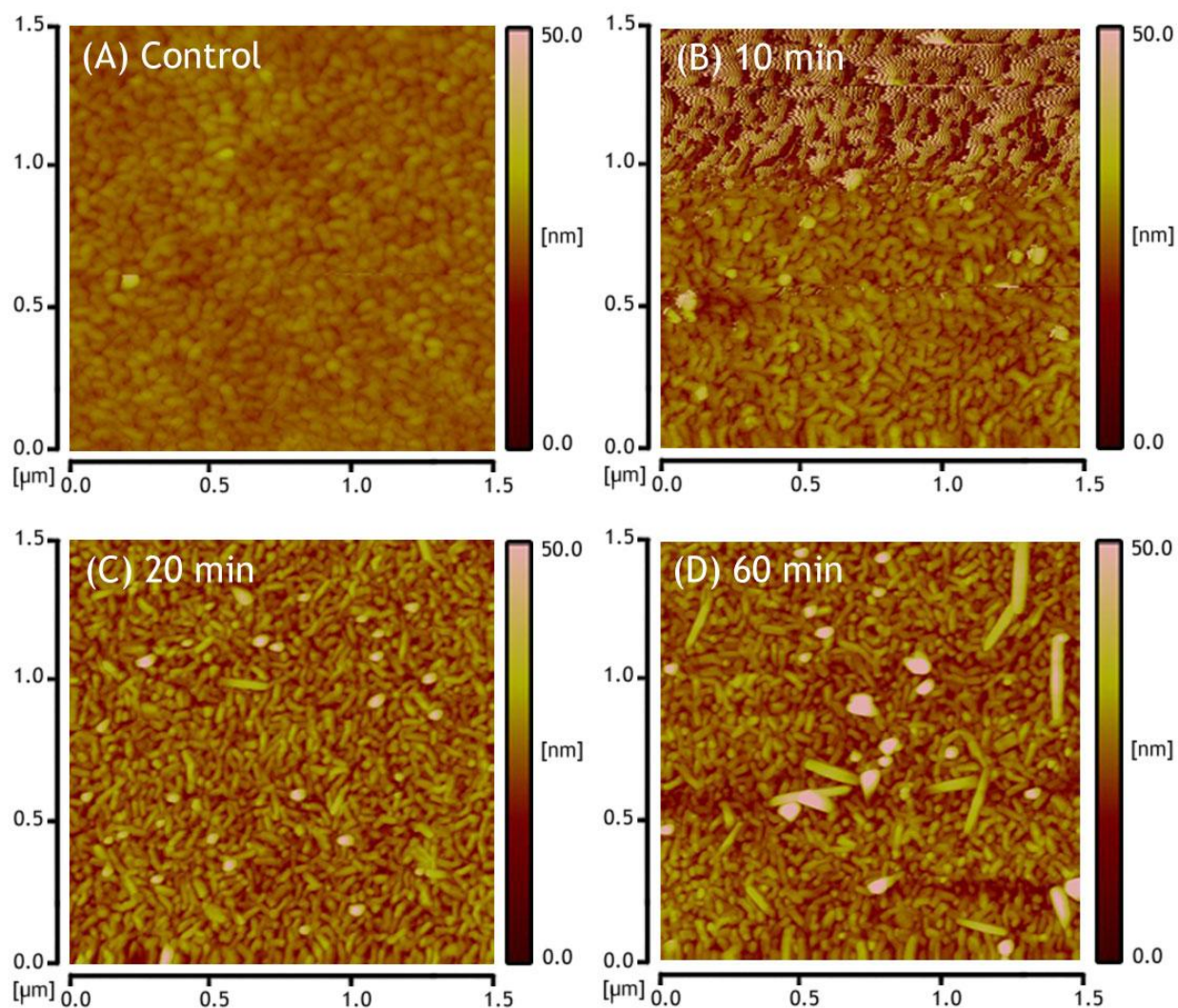


**Figure 3.1.1** - AFM Images of Acetone Treated CuPc Films: Each film is composed of 50 nm of CuPc deposited over 40 nm PEDOT:PSS and exposed to acetone vapor for (A) 0 min, (B) 10 min, (C) 20 min, and (D) 60 min.

### 3.2 ACETONE VAPOR TREATMENT

The acetone vapor treatment time was varied to determine whether device performance could be optimized by controlled nanorod growth. The nanostructured CuPc films were incorporated into OPV cells and analyzed for device characteristics. Values for device parameters listed are the average of 12 measurements, two solar cells with six electrodes each. Figure 3.2.1 shows the efficiency data. For times less than 15 min, the efficiencies are unchanged compared to the control cell, within error (standard

deviation over all electrodes for two devices is displayed). At 15 minutes, there appears to be a step increase in efficiency, then a gradual drop in efficiency at times longer than 40 minutes. Referring to the AFM images, it can be seen that the first nanorods form about 15 min, and continue to grow as the treatment time increases; therefore, this enhanced efficiency is not likely the result of increased nanorod size alone, or increasing efficiency would continue to be seen with increasing treatment time. Previous studies have shown that once nanorods reach a very large size (several hundreds of nanometers in length), continued exposure to solvent vapor can cause the nanorods to degrade into a disordered film [4]. It could be that nanorod growth and exposure of the organic film to open air (including oxygen and water vapor) are at odds with each other, causing a maximum efficiency when nanorods form, but before prolonged water vapor exposure and degradation can take effect. An increase in current leakage could also be causing decreased efficiency at higher treatment time (discussed below).

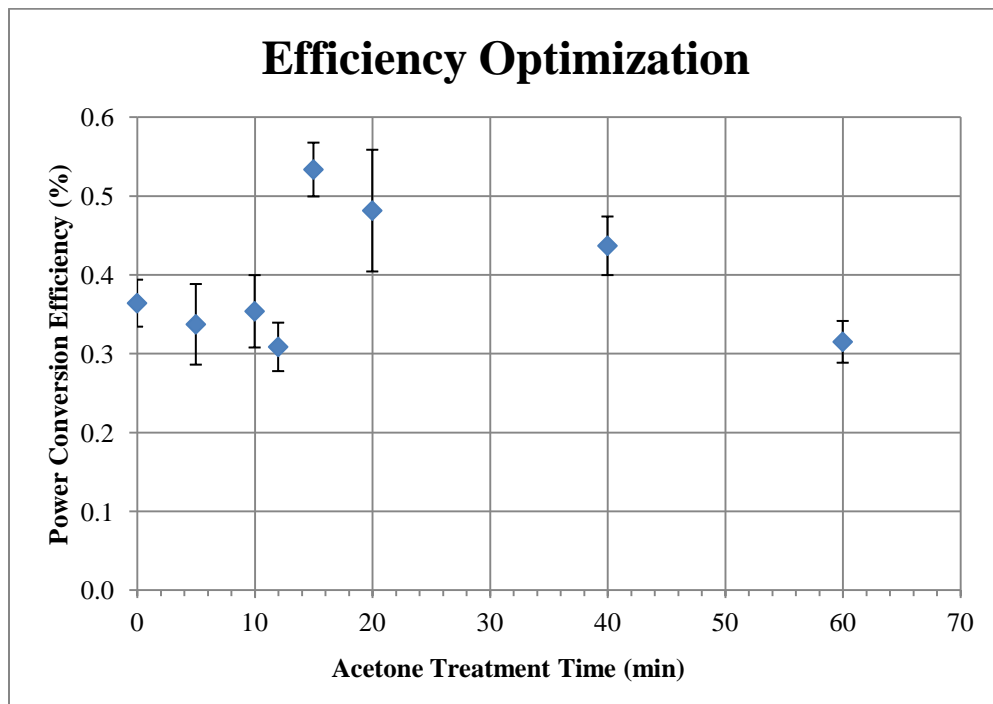


Figure 3.2.1 - Efficiency Optimization by Acetone Vapor Treatment:

The raw current-voltage data collected from the treated OPV cells can be found in Appendix B. Table 3.2.1 shows the device properties calculated by the Oriol PVIV software. Figures 3.2.2 and 3.2.3 show the same data in a graphical format. While the open circuit voltage and fill factor for the OPV cells do show



variation in performance, there does not appear to be a clear trend with respect to acetone treatment time. It should be noted that the exceptionally high fill factor for the 40 min cells may be anomalous; The 40 min cell was fabricated using a ITO-glass substrate from a different batch than the rest of the cells. If the 40 min fill factor anomaly is ignored, the graph indicates that both open circuit voltage and fill factor experience a slight increase after nanorod formation at 15 min. The largest contribution to the increase in efficiency after nanorod formation is the short circuit current. Introducing CuPc nanorods into the donor-acceptor interface was intended to decrease the exciton diffusion path length to the interface, with the effect of reducing current and voltage loss to recombination. As seen in Figure 3.2.3 , the current varied greatly between electrodes on each cell, giving large standard deviations for each. For the 15 min cell, the short circuit current density experienced a positive increase, but it just barely falls within the error of the 12 min cell, meaning the increase may not be statistically significant. Likewise, the current density of all cells after 15 min fall within error of the neighboring cells; therefore, improvement of current density by CuPc nanorods within these OPV cells is questionable.

**Table 3.2.1 - Analysis of Acetone Vapor Treatment**

<b>Treatment Time</b>	<b>V<sub>OC</sub> (v)</b>	<b>J<sub>SC</sub> (mA/cm<sup>2</sup>)</b>	<b>FF (%)</b>	<b>Efficiency (%)</b>
0 min	0.490 ± 0.011	2.10 ± 0.19	31.4 ± 1.0	0.364 ± 0.030
5 min	0.402 ± 0.062	2.42 ± 0.18	29.9 ± 2.3	0.337 ± 0.051
10 min	0.424 ± 0.018	2.36 ± 0.18	30.1 ± 4.0	0.354 ± 0.046
12 min	0.386 ± 0.010	2.31 ± 0.27	30.3 ± 1.8	0.309 ± 0.031
15 min	0.478 ± 0.020	2.80 ± 0.23	35.5 ± 1.5	0.534 ± 0.034
20 min	0.474 ± 0.029	2.54 ± 0.42	35.9 ± 1.8	0.482 ± 0.077
40 min*	0.359 ± 0.005	2.51 ± 0.31	46.1 ± 2.2	0.437 ± 0.037
60 min	0.381 ± 0.008	2.23 ± 0.28	33.3 ± 1.9	0.315 ± 0.027

Data from single cell only. Substrate from a different batch, from Thin Films Inc. ITO may be different

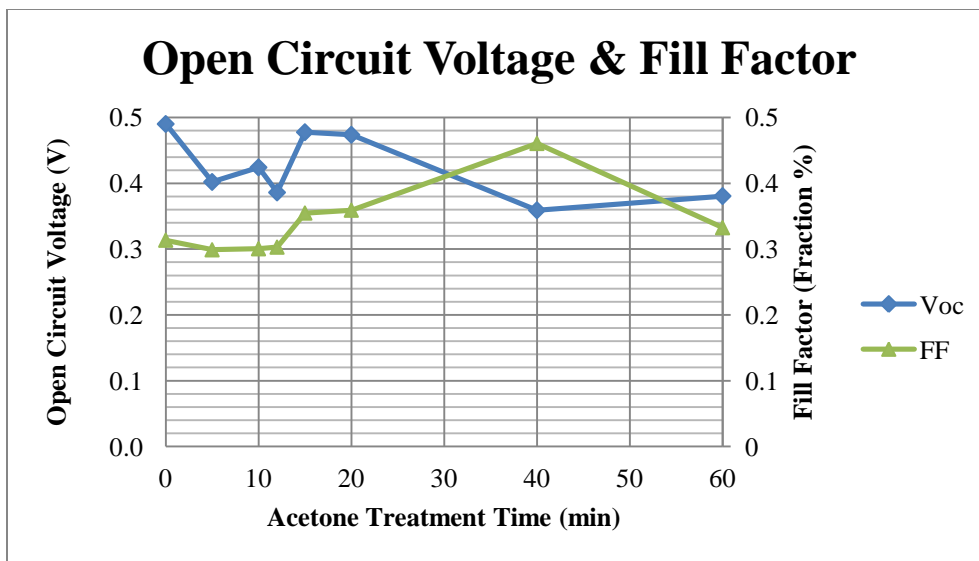


Figure 3.2.2 - Acetone Treated Devices, Open Circuit Voltage & Fill Factor

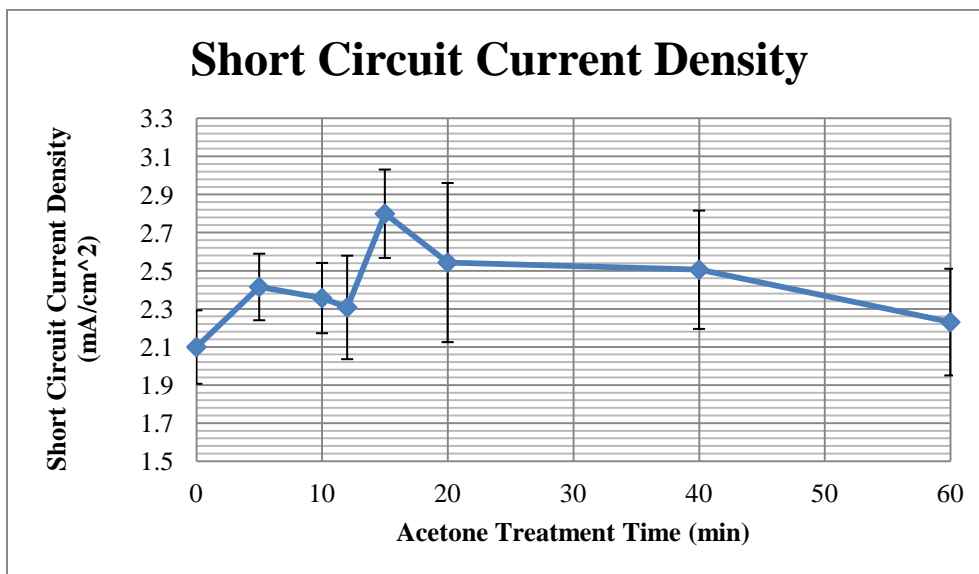


Figure 3.2.3 - Acetone Treated Devices, Short Circuit Current Density

Several factors could have contributed to the lower-than-predicted short circuit current density and overall efficiency for these cells. For one, the open circuit voltage ought to have remained roughly constant throughout all treatment times, due to the fact that the open circuit voltage is a function of the energy difference between the HOMO of the donor and the LUMO of the acceptor in an OPV [1]. Recombination of excitons is a factor that can cause a decrease in open circuit voltage in OPV cells. Instead, a higher open circuit voltage is observed in the control cell compared to the 5-12 min range cells.

If the organic films are experiencing oxidation/degradation during the acetone vapor treatment, this could cause a decay in open circuit voltage, with the formation of nanorods causing a partial recovery of open circuit voltage when recombination is reduced.

Other current and voltage losses may be due to the nanorods themselves. Figure 3.1.1 shows vertical nanorods with a height of 50 nm at treatment times of 20 min and higher. Considering that the C<sub>60</sub> acceptor layer deposited on top of the CuPc film is only 40 nm thick, it is possible that CuPc nanorods penetrate the C<sub>60</sub> layer, making contact with the BCP layer above. This would cause current leakage between the electrodes. Current leakage due to excessive nanorod height may explain why the short circuit current density does not significantly change with increasing surface roughness and nanorod size, which both normally contribute to reduced recombination and increased current generation. Additionally, since thermal deposition was used to apply the C<sub>60</sub> layer, the three-dimensional geometry of the CuPc nanorods may have interfered with the deposition. The C<sub>60</sub> layer may not infiltrate areas shadowed by the nanorods. This would cause voids within the active layer, which typically result in a decrease in fill factor.

### 3.3 SOLUBILITY PARAMETER APPROXIMATION

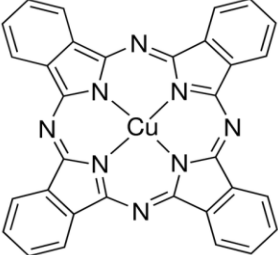
The solvent properties that lead to successful nanorod formation and interface roughness were examined. Previous studies seem to suggest that liquid drop volume is proportional to nanorod size [3]. For a vapor treatment, one may think the vapor pressure of the solvent would be a reasonable analog for quantity of solvent able to make contact with the CuPc surface. This is because the equilibrium partial pressure of solvent vapors in the annealing chamber would be proportional to the solvent's vapor pressure. Additionally, the rate of evaporation of a solvent is vapor pressure dependent, which is promising because nanorod formation has been observed to occur during solvent evaporation during liquid drop treatment [3]. However, comparison of solvent vapor pressure values to treated OPV efficiency of past studies did not reveal a pattern [8]. Seeking properties that may describe the solvents ability to interact with CuPc, parameters such as polarity were compared as well, but again no pattern was found.

Instead, the Hildebrand solubility parameter was chosen as the likely property to correlate with the growth of CuPc nanorods. The Hildebrand solubility parameter, despite being designed for solution mixing, has been shown to correlate to such diverse properties as boiling point, wettability, surface tension, and glass transition temperature in polymers [10]. When selecting a solvent for maximum solubility of an organic material, the solubility parameter of the solvent must match that of the organic precisely, as the solubility drops off near exponentially as one deviates from the maximum [11]. Therefore, in order to choose a solvent to maximize CuPc solubility, surface interaction, and hopefully nanorod formation, the Hildebrand solubility parameter of CuPc must be approximated. The solubility parameter is simply a measure of the cohesive energy density of a molecule, or  $\delta = (\Delta E / V)^{1/2}$ , where  $\Delta E$  is the energy of vaporization and  $V$  is the molar volume [10]. Rather than experimentally determining the  $\Delta E$  and  $V$  for an organic compound, Fedors describes the group contribution method, which uses the individual atomic contributions of structural groups in a molecule to find the energy of vaporization and molar volume [10]:

$$\text{Hildebrand Solubility Parameter, } \delta = \left( \frac{\sum \Delta e_i}{\sum \Delta v_i} \right)^{1/2}$$

This allows the approximation of the Hildebrand solubility parameter of an organic compound based solely on its structure, by finding the group contributions in convenient reference tables [12]. The group contribution method does have a few caveats. Firstly, atomic position in the chemical structure does not affect the parameter; however, since CuPc is largely symmetrical, the error should be small. Secondly, the energy of evaporation for metal groups is not well studied, as the method was developed for organic compounds, which presents a larger problem. The inability to account for the copper atom in the calculation was recognized by expecting some inaccuracy in the parameter's value. Since the copper atom is shielded symmetrically by the phthalocyanine groups, it is assumed that the molecule's interactions are mostly governed by the phthalocyanine group. Since the heat of vaporization of metals are usually very large relative to nonmetals, it can be expected that this estimation of the solubility parameter will be low.

Table 3.3.1 shows the contribution of each atom to the solubility parameter, which was calculated to be roughly 25 MPa<sup>1/2</sup>.

Structure	Count (n)	$\Delta e_i$ (cal/mol)	$n \times \Delta e$	$\Delta v_i$ (cm <sup>3</sup> /mol)	$n \times \Delta v$	
-CH=	4	1030	4120	13.5	54	
C=	10	1180	11800	16.1	161	
Disubst. Phenyl	3	7630	22890	52.4	157.2	
N	2	1000	2000	-9	-18	
-N=	6	2800	16800	5	30	
Cu	1	??	??	??	??	
			TOTAL:	~57610	TOTAL:	~384.2
			Hildebrand Solubility Parameter:		~25.09 MPa <sup>1/2</sup>	

Examination of the solubility parameters of solvents used in CuPc growth by previous studies reveal that the solvents all have a parameter of about 18-20 MPa<sup>1/2</sup> (Table 3.3.2). As aforementioned, the solubility of an organic has a very narrow range of parameters allowed for maximum solubility, therefore this sample range was inadequate. Given that the solubility parameter of CuPc was calculated to be around 25 MPa<sup>1/2</sup>, solvents with higher parameters were desired. Ethanol was selected as a solvent that closely matches CuPc's own value, and dimethyl sulfoxide (DMSO) was selected as upper value since the approximation was expected to be an underestimate.

Chemical	$\delta$ (MPa <sup>1/2</sup> )	Chemical	$\delta$ (MPa <sup>1/2</sup> )
Chloroform	19.0	Acetone	20.3
Chlorobenzene	19.4	Ethyl Alcohol	26.0
Toluene	18.2	DMSO	29.7

### 3.4 OTHER SOLVENT RESULTS

Since the treatment time that led to the peak cell efficiency in acetone vapor treated cells was 15 min, that time was chosen to test the selected solvents. Treatment method was kept exactly the same, as described in the Device Fabrication section. Figure 3.4.1 below shows the new treated thin films side by side with the 15 min acetone treated surface from the previous experiment.

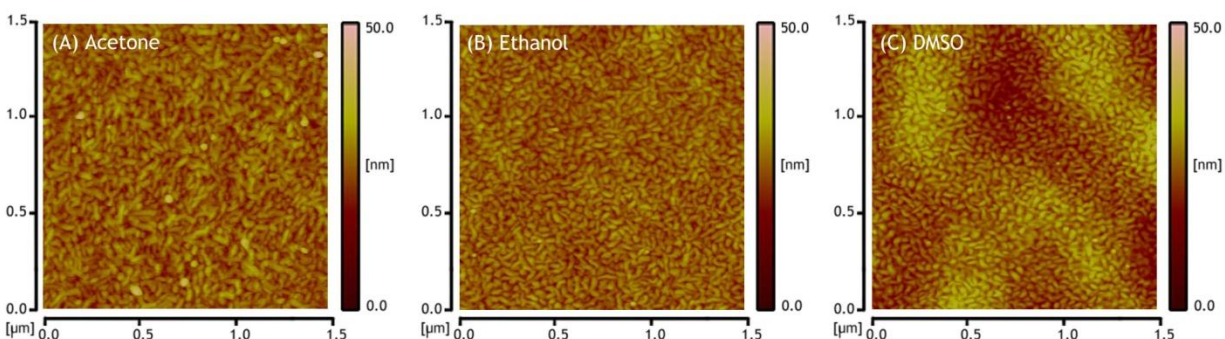


**Figure 3.4.1** - AFM Images of Other Solvent Treatments

A comparison of the surface roughness,  $R_a$ , of the above films is as follows: Acetone, 2.48 nm; Ethanol, 2.28 nm; and DMSO, 3.41 nm. The ethanol treated surface looks to be similar to the untreated CuPc surface (see Figure 3.1.1) with slight merging of the CuPc beads. The DMSO treated surface on the other hand displays wide regions of elevated CuPc, and an overall higher degree of variation in film height. Examining Table 3.4.1, the increased surface roughness appears correlated with cell efficiency, as one would expect. The fill factor of the DMSO is much higher than the acetone and ethanol treated cells. Interestingly, one would expect the improved surface roughness would cause a decrease in recombination, and thus an increase in device current; however, the current densities of the ethanol and DMSO cells are the same, within error.

Treatment	$V_{OC}$ (v)	$J_{SC}$ ( $\text{mA}/\text{cm}^2$ )	FF (%)	Efficiency (%)
Acetone	$0.478 \pm 0.020$	$2.80 \pm 0.23$	$35.5 \pm 1.5$	$0.534 \pm 0.034$
Ethanol	$0.377 \pm 0.006$	$2.26 \pm 0.13$	$29.8 \pm 1.1$	$0.289 \pm 0.009$
DMSO	$0.401 \pm 0.008$	$2.34 \pm 0.21$	$48.0 \pm 1.4$	$0.505 \pm 0.039$

The DMSO treatment appears to cause significant improvement of the surface roughness and efficiency compared to the untreated cell. The 35% improvement of the fill factor of the DMSO treated cell compared to the acetone treated cell indicates that further exploration of DMSO treatment should be explored. Since the 15 minute treatment time was optimized for acetone, it is expected that optimization of DMSO treatment times would yield a cell with efficiency better than that of any acetone treatment.

Table 3.4.2 shows the vapor pressures of the solvents used in this experiment. Acetone's vapor pressure is much higher than that of ethanol and DMSO; however, variation in the surface roughness of the CuPc films was observed for all of the treatments. This confirms that DMSO had a partial pressure in the annealing chamber at least high enough to cause interaction with the surface, and ultimately improvement of device characteristics. The less developed nanorods that were observed for the ethanol and DMSO treated films, compared to the well developed nanorods in the acetone treatment, may be attributed to the lower vapor pressure, however. This all the more suggests that DMSO had a much greater interaction with the surface, since it was able to cause comparable device efficiency even at very lower partial pressures. It should be noted that no nanostructuring was observed in any films due to prolonged exposure to open air; all devices were kept in open air for several hours during AFM imaging, yet the untreated CuPc still showed the planar/beaded surface typical of a thermally evaporated film.

<b>Chemical</b>	<b>Vapor Pressure at 25°C</b>
Acetone	230.04 mmHg
Ethanol	58.71 mmHg
DMSO	0.62 mmHg

## 4 CONCLUSIONS

In conclusion, a nanostructured CuPc film with peak heights of at least 50 nm was achieved, and a region of improved device efficiency found for acetone treatment times between 15-40 minutes. The maximum power conversion efficiency, at 15 min of treatment time, was 0.534%, which is a 46.5% improvement

versus the untreated cell (efficiency 0.364%). However, the ITO/PEDOT/CuPc/C<sub>60</sub>/BCP/Al cells completed using dry methods only showed a degradation in device properties while the nanorods were still observed to be growing. Efficiencies achieved were significantly lower than comparable ITO/PEDOT/CuPc /PCBM/BCP/Al devices fabricated in other studies, in which the acceptor layer (PCBM) was applied by solution processing (typical efficiency 1.5-3.0%) [8]. Deposition of the acceptor layer by thermal evaporation may have inadequately filled the CuPc nanostructure spacing due to 3D shadowing effects of the CuPc nanorods. Additionally, vertical CuPc nanorods of 50 nm or higher may have induced current leakage by penetrating the C<sub>60</sub> layer, and providing a path for carriers to travel to the cathode in reverse of photocurrent.

Moreover, the Hildebrand solubility parameter,  $\delta$ , was shown to be a practical means of selecting a solvent with high CuPc solubility, and surface interaction. The group contribution method predicted the solubility parameter to be at least 25.09 MPa<sup>1/2</sup>. The presence of the copper atom suggested that the parameter would have a higher true value. Ethanol ( $\delta = 26.0$  MPa<sup>1/2</sup>) was observed to have a poor effect on the CuPc surface, which showed very little improvement in CuPc nanostructuring. In all likelihood, ethanol would have an effect similar to acetone if the treatment time was optimized, since its solubility parameter is closer to CuPc's true value; however, the DMSO ( $\delta = 29.7$  MPa<sup>1/2</sup>) treatment was immediately indicative that interaction with the CuPc was improved. DMSO was found to raise device efficiency to 0.5054%, with a significantly higher fill factor than the acetone treatment, owing to a sharply decreased series resistance. Suggestions regarding further examination of DMSO may be found below.

## 5 FUTURE STUDIES

DMSO shows much promise as an annealing solvent. Without optimization of the treatment time, the DMSO treated device approached (matched, within error) the highest efficiency that was achieved with acetone treatment. Furthermore, a much higher fill factor (48.0% compared to 35.0%) was observed as a



result of a substantially reduced series resistance. It is currently unclear how the solvent could change the series resistance so dramatically. Future experiments should be conducted with varying DMSO treatment time to determine how the growth of CuPc nanorods differ when compared to acetone. The mechanism by which DMSO causes a decrease in series resistance should also be examined. Lastly, solvents with Hildebrand solubility parameters higher than  $29.7 \text{ MPa}^{1/2}$  should be studied as CuPc annealing solvents, to obtain insight into the precise solubility parameter of CuPc. A comprehensive study could instead examine CuPc's solubility in solvents with a wide range of solubility parameters, to obtain an exact value.

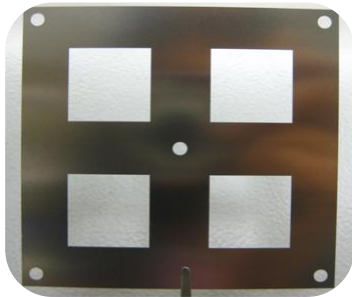
## BIBLIOGRAPHY

1. Nayak, PK, Bisquert J, and Cahen, D, **Accessing Possibilities and Limits for Solar Cells**, *Advanced Materials* 23, 2011, 2870-2876
2. Shah, A.; Torres P.; Tscharnner R.; Wyrsh N.; H. Keppner, **Photovoltaic Technology: The Case for Thin Film Solar Cells**, *Science* 285, 1999, 692-698
3. Yan Xiao, Yan Li, Meng Zhang, Feng-Xia Wang, and Ge-Bo Pan, **Single-crystal Copper Phthalocyanine Nanorods Self-assembled by a Solvent Evaporation Method**, *Chem. Lett.* 2011, 40, 544-545
4. Hongxia Xi, Zhongming Wei, Zhiming Duan, Wei Xu, and Daoben Zhu, **Facile Method for Fabrication of Nanostructured CuPC Thin Films To Enhance Photocurrent Generation**, *J. Phys. Chem. C*, Vol. 112, No. 50, 2008
5. Hyejin Gong, Jinhyun Kim, and Sanggyu Yim, **Carrier Gas Assisted Solvent Vapor Treatment for Surface Nanostructuring of Molecular Thin Films**, *Bull. Korean Chem. Soc.* 2012, Vol. 33, No. 3
6. Andre Moliton and Jean-Michel Nunzi, **How to Model the Behavior of Organic Photovoltaic Cells**, *Polymer International* 55, 2006, 583–600
7. Paul W. M. Blom, Valentin D. Mihailetschi, L. Jan Anton Koster, and Denis E. Markov, **Device Physics of Polymer: Fullerene BHJ Solar Cells**, *Advanced Materials* 19, 2007, 1551-1566
8. S Karak, S K Ray and A Dhar, **Improvement of Efficiency in Solar Cells based on Vertically Grown Copper Phthalocyanine Nanorods**, *J. Phys. D: Appl. Phys.* 43 (2010) 245101
9. A.S. Yapi, L. Toumi, Y. Lare, G.M. Soto, L. Cattin, K. Toubal, A. Djafri, M. Morsli, A. Khelil, M.A. Del Valle, and J.-C. Bernède, **On the Influence of the Electron Blocking Layer on the Organic Multilayer Cells Properties**. *Eur. Phys. J. Appl. Phys.* **50**, 2010, 30403
10. Fedors, Robert F., **A Method for Estimating Both the Solubility Parameters and the Molar Volumes of Liquids**, *Polymer Science and Engineering*, Iss. 2, vol. 14, 1974, 147-154.

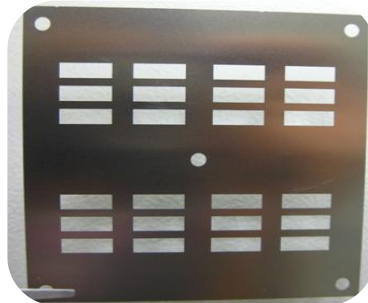
11. N. Sivaraman, R. Dhamodaran, I. Kaliappan,, T. G. Srinivasan, P. R. Vasudeva Rao, and C. K. Mathews, **Solubility of C<sub>60</sub> in Organic Solvents**, American Chemical Society, Journal of Organic Chemistry, 1992, 57, 6077-6079
12. Wilkes, C. E., J. W. Summers, C. A. Daniels, and Mark T. Berard. "**Solubility Parameter Values**" *PVC Handbook*. Cincinnati: Hanser/Gardner, 2005. 675-714. Print.
13. Lange, Norbert Adolph., and John Aurie. Dean. "**Vapor Pressures of Various Organic Compounds**" *Lange's Handbook of Chemistry*. 15th ed. New York: McGraw-Hill, 1998. N. pag. Print.

## APPENDIX A

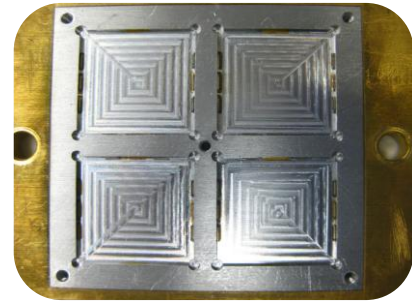
The following are the custom device fabrication and testing apparatuses used for OPV applications:



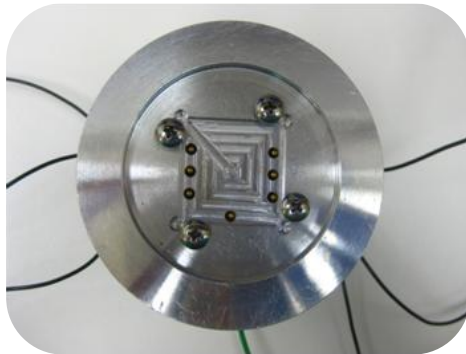
(a) Mask for active layer deposition  
(4 substrates)



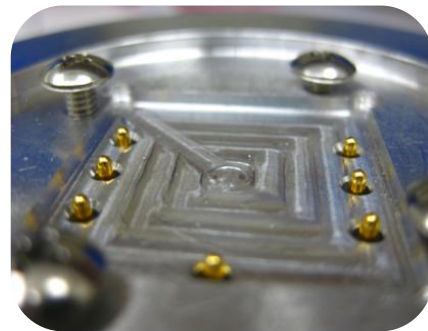
(b) Mask for electrode deposition  
(4 substrates)



(c) Loading base for thermal evaporation vacuum chamber



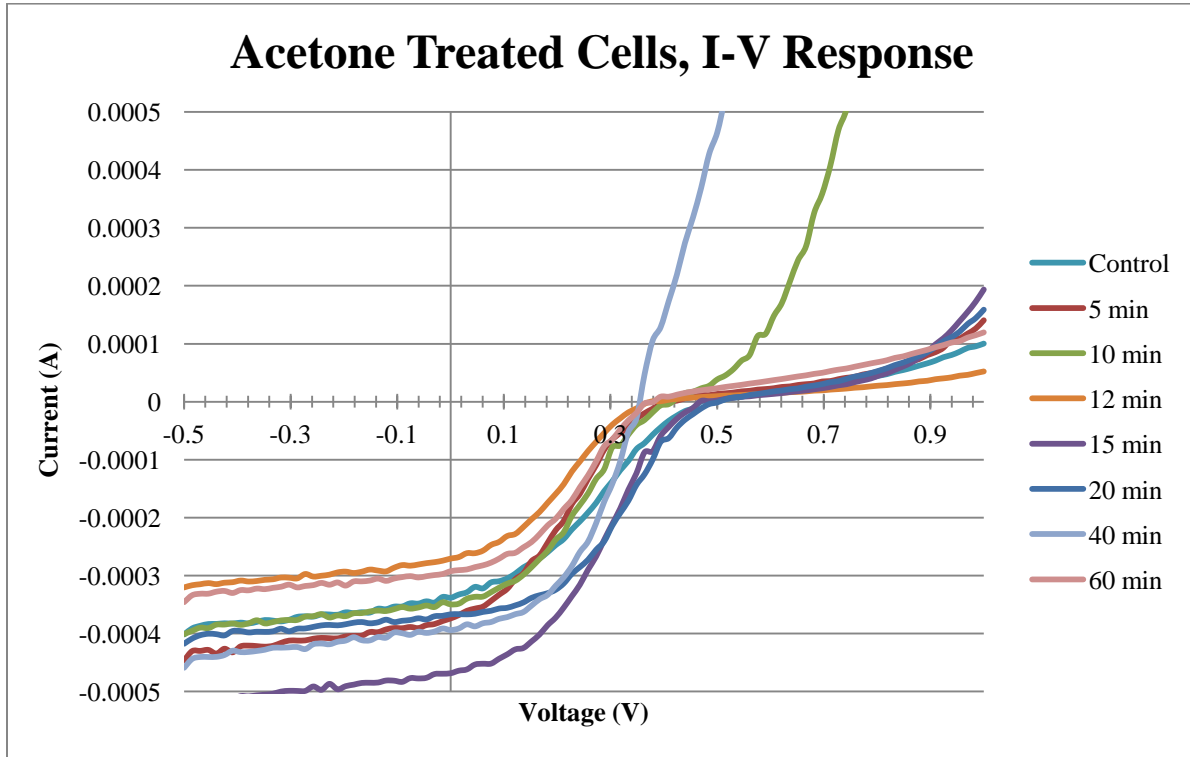
(d) OPV testing apparatus



(e) Contact pins for electrodes on testing apparatus

## APPENDIX B

The following is a comparison of the current-voltage response from the acetone vapor treated OPV cells:



The following is a comparison of the current-voltage response from the other solvent treated OPV cells:

